2018 IEEE-RAS 18th International Conference on Humanoid Robots (Humanoids)
Beijing, China, November 6-9, 2018

Implementation of Stable and Efficient Hopping with Serial Elastic Actuators

Yichao Mao[1], Jing Xu[2], Qiuguo Zhu[3], Jun Wu[4], Rong Xiong[5]

Abstract— **Inspired by biological systems, robots that exploit the natural dynamics of compliant joints are developed in recent years to obtain stable and efficient locomotion. In these robots, series elastic actuator (SEA) is widely used due to its compliant property and energy storage capacity. However, robots that are equipped with SEA have drawbacks of substantial delay and limited bandwidth. Additionally, high speed locomotion also engenders severe vibration and cause noise pollution in posture measurement of the robot. These inevitable features make the efficient robots hard to demonstrate precise control and perform dynamic balance. To cope with these problems, beside traditional hopping and foot hold selection algorithms, two methods are proposed in this paper for consecutive hopping: (1)a position controller which generates active damping to stabilize the joint position;(2)a learning algorithm for body balance control. The learning algorithm discretizes the continuous control problem into phases and adopts integration form of body dynamics to maintain balance. Instead of empirically tuning the control parameters, model identification and learning algorithms are employed to automatically tune these proposed controllers. Experiments were conducted on SEA based single leg robot by swinging leg between two demanded position and maintaining body balance during consecutive hopping. By combining the proposed algorithms, stable and efficient hopping was implemented.**

I. INTRODUCTION

Inspired by the motion pattern of biological systems, researches of legged robots have made progress in these years. One category is consisted of robots without compliant components in their joints. Traditional rigid robots which are built on a strong industrial background require highly elaborated motion planning to achieve stable locomotion[1], [2]. Besides, due to impact-robust and high power to weight ratio properties, the hydraulic actuators based humanoid and quadruped robots such as Boston-Dynamics's *BigDog*[3], *LS3*[4] or *HyQ*[5] exhibits significant versatility, robustness, and speed under high environmental disturbance and uncertainties. In spite of the success these robots have achieved, they are inefficient in energy consumption. An exception of such kind of robots is the *MIT Cheetah*[6], which equips high torque motors and low ratio reducers to achieve high performance of running and hopping, and employs capacitors to recycle energy. However, the actuators of the robot require custom design[7].

Addressing the importance of energy efficiency, high compliant components are used to build efficient legged robots which can perform stable locomotion with simple control algorithm[8], [9] and are more robust to interact with environmental uncertainties and disturbance[10]. To exploit the passive dynamics of spring-load system which is inspired by biological compliant element as tendon or muscle in human and quadruped animals, a lot of studies have been done and researches on efficient locomotion of hopping and running have made a great progress these years. R. Niiyama developed a bipedal hopping and landing robot *Mowgli* with pneumatic actuators and passive springs[11], S.H.Hyon built a hydraulic hopping robot *KenKen*[12] with a spring in passive ankle joint to achieve efficient hopping. Such robots are based on hydraulic or pneumatic actuators, but the requirement of external air compressor or hydraulic pump make these robot difficult to downsize.

Then, several prototypes of bipedal robots with serial elastic actuators (SEA)[13] are successfully achieved high performance on dynamic motions in recent years. By designing the stiffness and damping carefully, J. Hurst and J. W. Grizzle employed pulley systems and antagonistic spring systems to build efficient hopping robot *Thumper*[14] and running robot *MEBAL*[24] with variable compliance. The robots can perform walking and running on uneven terrain with high stability and controllable velocity. M. Hutter designed unified SEA to develop single leg robot *ScarlETH*[16], [17] for efficient and versatile locomotion, and successfully apply their unified leg prototype into their quadruped robot *StarlETH*[18]. Efficient hopping locomotion is demonstrated by their single leg prototype and various stable gaits are implemented on their quadruped robot. Grimmer built a hopping robot with SEA in ankle joint to reduce peak power and energy requirement of the actuators[19]. Other bipedal robot such as HUME[20], BIOBIPED[21], COMAN[22] or M2V2[23] are also equipped with SEA actuators to implement force control based algorithms. The SEA can be wielded as either a torque servo or position servo. Additionally, as a high power density element, the spring installed in the robot is used to decouple motor inertia and load inertia, eliminating the inelastic collision and the associated energy loss, restore and recycle the hopping energy[24].

Although benefits of robustness and efficiency have been achieved by applying SEA in the joints of robots, the intrinsic characteristics of SEA impose limitations to the performance

This work was supported by the National Nature Science Foundation of China (Grant No.NSFC: 51405430) and National Defense Innovation(Grant No.1716311XJ00100501)

Yichao Mao, Jing Xu, Qiuguo Zhu, Jun Wu and Rong Xiong are with the State Key Laboratory of Industrial Control and Technology, Zhejiang University, Hangzhou, P. R. China , Institute of Cyber-System and Control, Zhejiang University. Jun Wu are with Binhai Industrial Technology Research Institute of Zhejiang University, 300301, Tianjin, China. Qiuguo Zhu is the corresponding author. qgzhu@zju.edu.cn

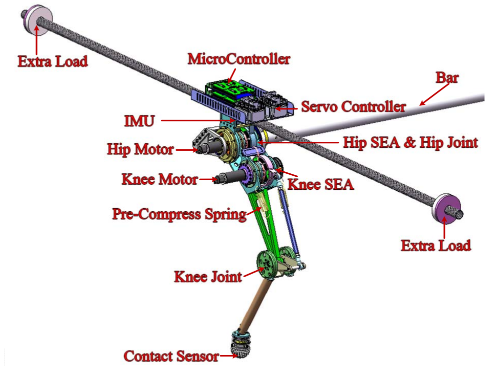

Fig. 1: Mechatronic system of single leg robot

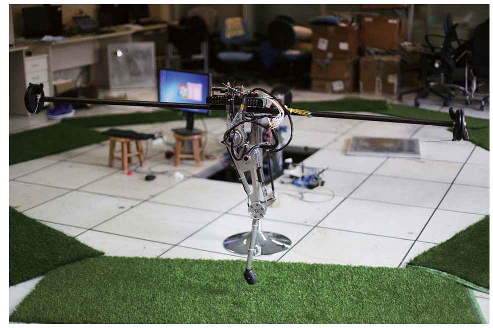

Fig. 2: Photograph of single leg robot

of joints and should be carefully investigated. The optimal passive dynamics of compliant joint and its mathematical model is analyzed by J. W. Hurst[25]. It points out that damping plays an important role in improving the performance of SEA by preventing re-bouncing and oscillation. While in *ScarlETH*, two methods were used to generate damping: the first one is to install damper and rely on the internal collision to reduce load energy, the second one is to introduce LQR controller to provide active damping to prevent the leg from oscillation[16], [17]. However, the control parameters were tuned empirically, and the body balance controller based on SEA was not mentioned in this paper.

In order to make the controller easy to adapt different robots, methods that can simplify and automate the tuning process are demanded. Hence, two auto tuned controllers are proposed in this paper: (1)a modified position controller is employed to control position of SEA joint by generating active damping; (2)a balance control algorithm to maintain body balance during consecutive hopping, which discretizes the continuous control problem into phases and adopts integration form of body dynamics. The main contribution of the proposed algorithms is their capability to employ model identification and learning algorithms to ease the pressure of repeated tuning, especially for such SEA based system in which spring stiffness always varies after being used for a long time. Experiments of position control and body maintenance validate the effectiveness of the proposed controller.

Remainder of the paper is organized as follows. Section II describes the system and main scheme of controller. Section III introduces the implementation position controller. Section IV explains the body balance maintenance algorithms. Section V demonstrates the experimental result. In Section VI, conclusions and future work are discussed.

II. System Description

A. The Design of Robot

The robot is composed of three linkages, body, thigh and shank. Two articulated SEA joints are used to control the motion of knee and hip joint of the robot, and a passive joint is configured to constrain the motion of body in sagittal plane. A parallel four-bar linkages mechanism is employed for motion transmission and allows placing knee motor close to the body. While the CoG of the whole robot is close to the axis of hip link, fast response and low energy loss are obtained through this mechanical design. A carbon fibre tube with extra loads is installed on the robot to increase the moment inertia of body. The mechatronic structure is shown in Fig.1. The photograph of the robot is shown in Fig.2.

To efficiently drive the robot and minimize the energy an actuator should provide during consecutive hopping, one important aspect is to fully exploit the passive dynamics of the robot. Hence the configuration of the robot should be selected carefully. Two 200W 4-pole Maxon motors are combined with 120:1 CSG harmonic reducers to actuate the knee and hip joint. The stiffness of hip joint and knee joint is selected to engender a natural frequency vibration of approximately 2Hz when the robot crash to the ground, which is close to hopping frequency of human beings. The detailed configuration of mechanical parameters which are calibrated by measuring and identification will be shown in Section V.

Each joint is equipped with two absolute encoders to measure the deformation of spring in SEA. An MEMS IMU is installed at the center of the body to measure the tipping angle(pitch), while a contact sensor is installed at the foot. When the robot moves forward or backward, it rotates about an vertical axis where an incremental encoder is installed to measure the velocity of the robot.

B. The Design of Controller

To control the robot, a real time control system is implemented on the robot. Maxon motor in each joint is controlled by an Elmo servo controller with 10kHz current loop and 1kHz velocity loop. Both controllers and encoders are connected to a micro-processor, which can directly sends velocity command to the servo controller and controls the compression of joint spring with 400Hz. A real time system monitors all the data transmitted by micro-processor, IMU and contact sensor, and implements high lever actions such as body balance control, Raibert flight algorithms and position control. To design and implement these controllers, definition of coordinate frame and the symbols of important parameters illustrated in Fig.3 and Tab.I are employed. The coordinate

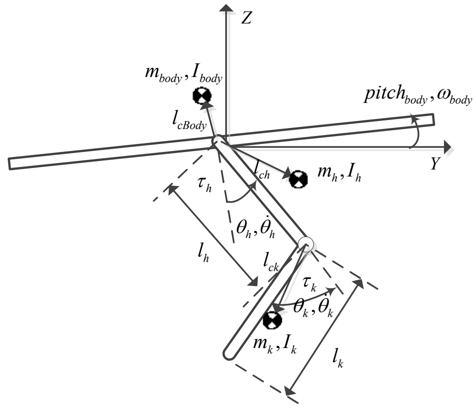

Fig. 3: Parameter definition of single leg robot

TABLE I: Definition of symbols in Fig.3

l_h	Length of the thigh
l_k	Length of the shank
l_{ch}	Distance between CoM of thigh and hip joint
l_{ck}	Distance between CoM of shank and knee joint
l_{cBody}	Distance between CoM of body and hip joint
K_{sh}	Spring stiffness of hip joint
K_{sk}	Spring stiffness of knee joint
K_{outer}	Spring stiffness of outer spring
θ_h	Angle of hip joint
θ_k	Angle of knee joint
$pitch_{body}$	Tipping angle of knee joint
ω_{body}	Tipping angular velocity of knee joint
m_h	Mass of the thigh
m_k	Mass of the shank
m_{body}	Mass of the body
I_h	Moment Inertial of the thigh
I_k	Moment Inertial of the shank
I_{body}	Moment Inertial of the body
K_{dh}	Damping ratio of hip joint
K_{dk}	Damping ratio of knee joint
τ_h	Torque of hip joint
τ_k	Torque of knee joint

frame takes the center of body as the origin, the axis of joint as X axis and the horizontal forward direction as Y axis.

The regulation of these controllers is totally event-based. When the robot takes off the ground and gets into flight phase, a foot hold selection algorithm which is proposed by Railbert in their early research is conducted to control the velocity of hopping[26]. Meanwhile, the position control algorithm is employed to move the joint to demanded position. When the robot contacts the ground and gets into stance phase, the hopping algorithm is started. Relying on the bouncing ability of an elastic robot, the injected energy is only required to compensate the energy loss of crash and damping. Hence a demanded position is sent to the knee motor to inject energy during stance phase. Meantime, body balance controller is activated to control the balance of body. All sampled data of the robot during hopping or other testing are recorded by the dynamics estimator which will calculate the dynamic parameters of robot offline to tune controllers. The whole control framework is shown in Fig.4.

III. SEA Joint Position Controller

Although SEA possesses advantages of low torque output noise and low energy loss when a robot crashes to the ground[14], traditional position control which is based on joint torque is hard to implement on SEA joints. Firstly, the limited bandwidth for torque output makes the joint difficult to track torque curve with high frequency. Secondly, as the torque controller of SEA is based on velocity control of joint motor[13], the control frequency is too low to satisfy the requirement of high speed response.

Hence, instead of using the joint torque to control joint position, the velocity of joint motor is selected as the control variable for the controller. However, directly sending a demanded position to joint motor will generate undesired oscillation and impairs the performance of position control. Thus, modification of demanded velocity of joint motor is required to eliminate the oscillation.

A position controller is proposed in this section due to the analysis above. While the damping ratio has a large stable range to select,parameters except the active damping ratio in the controller can be identified automatically based on the result of dynamic model identification.

As the shank of the robot is relative light compare to the thigh which is used to install both SEA of knee and hip, a leg of the robot during flight phase can be treated as a pendulum system. Moreover, as the inertia of body is much larger than the inertia of leg, we assume the body can be regarded as a rigid body without angular acceleration during consecutive hopping. The dynamics equation is:

$$I_l\ddot{\theta}_h + K_{dh}\dot{\theta}_h + m_l l_c sin(\theta_h + \theta_c)(g + a_{body}) = \tau_h \quad (1)$$

where I_l is the inertia momentum of the leg, m_l is the mass of the leg, l_c is the distance between CoG of the leg and the axis of hip joint, K_d is the damping of hip joint, θ_h is the angle position of hip joint, θ_c is the angle offset of the CoG when θ_h is zero, T is the torque of hip joint. g is the gravitational acceleration, a_{body} is the acceleration of the robot body.

Specifically, for the two-joint single leg robot, following equations are substituted to calculate the dynamics of leg:

$$m_l l_c \sin(\theta_h + \theta_c) = (\tilde{m}_h + \tilde{m}_k) l_h \sin(\theta_h) + \tilde{R}_{hy}\cos(\theta_h)$$
$$+\tilde{m}_k l_k \sin(\theta_h + \theta_k) + \tilde{R}_{ky}\cos(\theta_h + \theta_k) \quad (2)$$
$$I_l = \tilde{I}_h + \tilde{I}_k + \tilde{m}_k(l_h^2 + 2l_h l_k \cos(\theta_k)) - \tilde{R}_k y \sin(\theta_k) \quad (3)$$

where

$$\tilde{m}_h = m_h \frac{l_{ch}\cos(\theta_{ch})}{l_h} + m_k \frac{l_k - l_{ck}\cos(\theta_{ck})}{l_k} \quad (4)$$
$$\tilde{m}_k = m_k \frac{l_{ck}\cos(\theta_{ck})}{l_k} \quad (5)$$
$$\tilde{R}_{hy} = m_h \sin(\theta_{ch}) l_h \quad (6)$$
$$\tilde{R}_{ky} = m_k \sin(\theta_{ck}) l_k \quad (7)$$
$$\tilde{I}_h = I_h + m_h l_{ch}^2 + m_k \frac{l_k - l_{ck}\cos(\theta_{ck})}{l_k} l_h^2 \quad (8)$$
$$\tilde{I}_k = I_k + m_k l_{ck}^2 \quad (9)$$

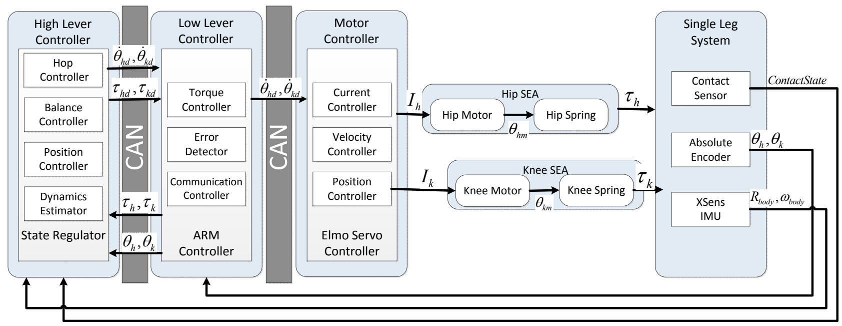

Fig. 4: Architecture of controller framework

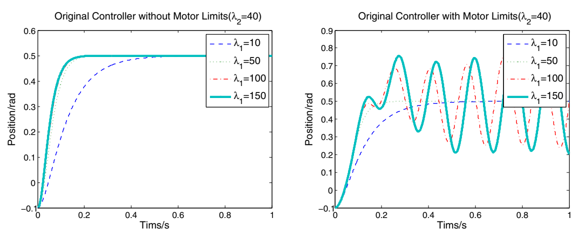

(a) (b)

Fig. 5: (a)Simulation results of controller without motor limits; (b)Simulation results of controller with motor limits

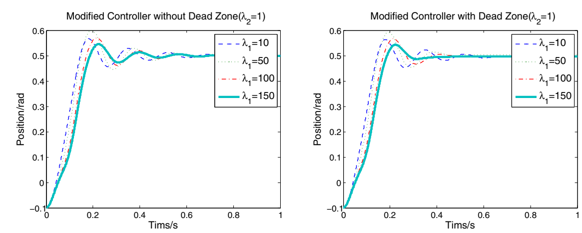

(a) (b)

Fig. 6: (a)Simulation results of controller without motor limits; (b)Simulation results of controller with motor limits

are the base parameters of this system and can be identified uniquely by dynamics identification algorithms. The definition of base parameters and dynamics identification algorithms are introduced in [27], [28].

In a SEA, the torque is represented by the compression of serial spring:

$$\tau_h = K_{sh}(\theta_{hm} - \theta_h) \tag{10}$$

where K_s is the stiffness of spring, θ_{hm} is the position of motor in hip joint. Based on the inner velocity loop of motor, we intend to control the position of joint θ_h to track a desire trajectory θ_{hd} by the velocity of motor $\dot{\theta}_{hm}$.

A combine error is introduced in the controller:

$$s = \lambda_1 \tilde{\theta}_h + \dot{\tilde{\theta}}_h \tag{11}$$

where $\tilde{\theta}_h = \theta_{hd} - \theta_h$ is the tracking error. To stabilize the system, following equation is designed to obtain the controller[29]:

$$\ddot{s} + 2\lambda_2 \dot{s} + \lambda_2^2 s = 0 \tag{12}$$

Substituting (1)-(11) into (12), the corresponding controller is deduced as:

$$\begin{aligned}\dot{\theta}_{hm} &= \dot{\theta}_h + K_{dh}/K_{sh}\ddot{\theta}_h + m_l(g + a_{body})l_c cos(\theta_h + \theta_c)\dot{\theta}_h \\ &+ \frac{I_l}{K_{sh}}\left((\lambda_1 + 2\lambda_2)\ddot{\tilde{\theta}}_h + (2\lambda_1 + \lambda_2)\lambda_2\dot{\tilde{\theta}}_h + \lambda_2^2\tilde{\theta}\right)\end{aligned} \tag{13}$$

where the parameter λ_1 and λ_2 are manually configured value to determine the poles of the system.

In Fig.5a, it is shown that when the the velocity $\dot{\theta}_{hm}$ and acceleration $\ddot{\theta}_{hm}$ are not limited, the global convergence of the controller is guaranteed. However, in robotic systems the capacity of motor is limited, which bounds the maximum value of acceleration or velocity the servo controller can demand. These limitations cause unexpected oscillation if the parameters are not selected carefully. In Fig.5b, it is shown that when λ_1 is selected as 100 or 150, the system controller engenders oscillations. Besides, the feedback of the load velocity $\dot{\theta}_h$ is unstable when measurement noise and output delay exist in the systems. To deal with such problem, a modified form of the controller is proposed by simply change (13) into:

$$\begin{aligned}\dot{\theta}_{hm} =& \dot{\theta}_{hd} + K_{dh}/K_{sh}\ddot{\theta}_h + m_l(g + a_{body})l_c cos(\theta_h + \theta_c)\dot{\theta}_h \\ &+ \frac{I_l}{K_{sh}}\left((\lambda_1 + 2)\ddot{\tilde{\theta}}_h + (2\lambda_1 + 1)\dot{\tilde{\theta}}_h + \tilde{\theta}\right)\end{aligned} \tag{14}$$

where the first term $\dot{\theta}_h$ in (13) is modified to $\dot{\theta}_{hd}$ to avoid self-excited oscillation, and fix the value of λ_2 to 1 to lessen the feedback gain. The required accuracy θ_{err} of the joint is set to be a dead zone for the controller to prevent oscillation near the demand position. The demand value of $\dot{\theta}_{hd}$ and $\ddot{\theta}_{hd}$ outside the dead zone is calculated by:

$$\triangle\theta_h = \theta_{hd} - \theta_{hm} + \frac{m_l(g + a_{body})l_c sin(\theta_{hd} + \theta_c)}{K_s} \tag{15}$$

$$\dot{\theta}_{hd} = \sqrt{2\ddot{\theta}_{hd}\left|\triangle\theta_h - \theta_{err} sgn(\triangle\theta_h)\right|} sgn(\triangle\theta_h) \tag{16}$$

In control system, the controller is initialized and bounded by:

$$\dot{\theta}_{hd}(0) = \dot{\theta}_h \tag{17}$$

$$\dot{\theta}_{hd}(k)=\begin{cases} \dot{\theta}_{hd}, & \left(\ddot{\theta}_{hd} < a_{set}\right) \quad (18a) \\ \dot{\theta}_{hd}(k-1)+a_{set}dt, & \left(\ddot{\theta}_{hd} > a_{set}\right) \quad (18b) \\ \dot{\theta}_{hd}(k-1)-a_{set}dt, & \left(\ddot{\theta}_{hd} < -a_{set}\right) \quad (18c) \end{cases}$$

$$\ddot{\theta}_{hd}(k)=\begin{cases} \frac{\dot{\theta}_{hd}(k)-\dot{\theta}_{hd}(k-1)}{dt}, & \left(\ddot{\theta}_{hd} < a_{set}\right) \quad (19a) \\ a_{set}, & \left(\ddot{\theta}_{hd} > a_{set}\right) \quad (19b) \\ -a_{set}, & \left(\ddot{\theta}_{hd} < -a_{set}\right) \quad (19c) \end{cases}$$

A trajectory with acceleration a_{set} is generated by this controller. As the position of each joint does not require high precision for force based robot, the algorithm make the controller more stable by sacrificing position accuracy. The simulations shown in Fig.6 indicates that the dead zone of the controller improves stability of position control.

For a practical system, dynamic parameters of the robot are not precisely equal to computed value of mechanical design. To implement the controller, dynamics identification algorithm[28] is adopted to calculate the value of leg dynamics. After identification, only the parameter λ_1 which indicates active damping ratio requires manual configuration, while a wide range for this parameter can stabilize the controller.

IV. Body balance maintenance

For a robot with high compliant SEA hip joint, the substantial dynamics and the capacity of actuators imposes limitation on the performance of torque output, and pose various challenges for us to implement traditional algorithms. In traditional hopping strategy, a simple PD controller is employed to maintain body balance. For an SEA based hip joint, several problems confine the use of a PD controller: (1) a short period exists after the robot crashes to the ground, during which the joint torque is uncontrollable; (2) the natural dynamics of the hip joints causes delay and bandwidth limitation in torque output; (3) the hopping engenders severe vibration and pollutes the measurement of body posture $pitch_{body}$ and angular velocity ω_{body}.

Fortunately, two properties of body balance maintenance problems inspire the design of a new controller. Firstly, the control of body balance is only conducted during stance phase. Hence, if the robot takes off the ground with large rotating velocity of body, the robot will tip severely and require large torque to push the body back. Secondly, it is observed that during each flight phase, the pitch angle of body varies in an approximately constant velocity. Hence, instead of measuring and controlling angle and angular velocity of body at every instant, the average angular velocity during flight phase can be chosen as the objective of the controller.

Based on the analysis above, instead of a continuous control problem, the issue of body balance maintenance is regarded as a discretized problem. The objective is to control the average velocity of body rotation during flight phase. To achieve the objective, the integration of hip torque during stance phase is employed to control the rotation. The model to calculate the demanded integration value of hip joint during stance phase can be fitted by the sampled data during hopping. Hence. instead of manually tuning, the controller is learned after several successful or failed hops. The scheme of the body balance controller is shown in Fig.7.

The value of average angular velocity of n^{th} hop $\bar{\omega}_{body}(n)$ is calculated by:

$$\bar{\omega}_{body}(n) = \frac{pitch_{fly}(n) - pitch_{crash}(n+1)}{t_{fly}(n) - t_{crash}(n+1)} \quad (20)$$

where $pitch_{fly}(n)$ is the pitch angle of body at n^{th} take-off of hopping, $t_{fly}(n)$ is the time of n^{th} take-off, $pitch_{crash}(n)$ is the pitch angle of body at n^{th} crash of hopping, $t_{crash}(n)$ is the time of n^{th} crash.

The dynamics equation of body during stance phase is:

$$I_{body}\dot{\omega}_{body} = m_{body} l_{cBody} \sin(pitch_{body})(g + a_{body}) - \tau_h \quad (21)$$

Instead of (21), the integration form of dynamic equation is used to control the average angular velocity $\bar{\omega}_{body}(n)$. As l_{cBody} and $pitch_{body}$ is small when the robot is not tipping, the change of angular velocity between two adjacent flight phase is proportional to the integration of hip torque during stance phase. More generally, a polynomial function $f(.)$ is employed to represent this equation:

$$\bar{\omega}_{body}(n) - \bar{\omega}_{body}(n-1) = f\left(\int_{t_{crash}(n)}^{t_{fly}(n)} \tau_h(t)dt\right) \quad (22)$$

where τ_h is the torque of hip joint. The function $f(.)$ is fitted by the data sampled from experiments.

To maintain the body balance, the demanded angular velocity for the next flight phase is calculated by the pitch angle of robot body:

$$\omega_{demand}(t) = \frac{pitch_{body}(t) - pitch_{set}}{t_{flight}} \quad (23)$$

where $pitch_{set}$ is the set value of body posture, $pitch_{body}$ is the measurement of pitch angle of robot body, t_{flight} is the time duration of flight phase, which is determined by experiments. Then the set value of integration of hip torque of n^{th} stance phase is calculated by:

$$Int_{hip}(t) = f^{-1}\left(\omega_{demand}(t) - \bar{\omega}_{body}(n-1)\right) \quad (24)$$

To achieve the integration value of hip torque, an online plan algorithm is designed to calculate the demand torque of hip joint:

$$\triangle Int_{hip}(t) = Int_{hip}(t) - \int_{t_{crash}(n)}^{t} \tau_h(t)dt \quad (25)$$

$$\tau_{hd} = \sqrt{2\dot{\tau}_{hd}\left|\triangle Int_{hip}(t)\right|} sgn(\triangle Int_{hip}(t)) \quad (26)$$

where $\triangle Int_{hip}(t)$ is the residue of demanded torque integration, τ_{hd} is the demanded torque of hip joint, $\dot{\tau}_{hd}$ is the bound of torque variation to limit the bandwidth of demanded torque.

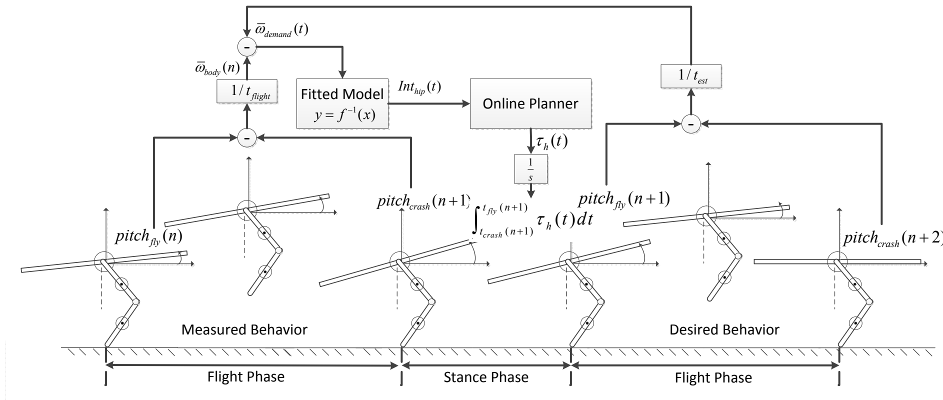

Fig. 7: Scheme of body balance controller during consecutive hopping

TABLE II: Configuration of robot

Parameter	Value	Calibration Method
l_h	$0.342m$	Measuring
l_k	$0.324m$	Measuring
l_{cBody}	$0.081m$	Measuring
K_{sh}	$212.1Nm/rad$	Measuring
K_{sk}	$172.3Nm/rad$	Measuring
K_{outer}	$33.16Nm/rad$	Identification
$\tilde{m}_h$	$2.432kg$	Identification
$\tilde{m}_k$	$0.293kg$	Identification
$m_{body} + m_k + m_h$	$13.61kg$	Measuring
$\tilde{R}_{hy}$	$0.0805kg.m$	Identification
$\tilde{R}_{ky}$	$0.0012kg.m$	Identification
$\tilde{I}_h$	$0.2686kg.m^2$	Identification
$\tilde{I}_k$	$0.0497kg.m^2$	Identification
I_{body}	$3.502kg.m^2$	Identification
K_{dh}	$0.2686Nm.s/rad$	Identification
K_{dk}	$0.1523Nm.s/rad$	Identification

According to the control algorithm of SEA prototype in [13], a PD controller of inner velocity loop with compensation of joint velocity feedforward is applied to implement precise torque output. Low noise and high disturbance rejection is achieved in this SEA based joint, while a substantial delay in tracking of a step set point is presented.

V. Experimental results

A. Calibration of Robot Dynamics

To implement proposed controllers, the calibration of dynamic parameters is conducted firstly. The weight of robot, length of each link and the stiffness of joint spring are measured directly, other dynamic parameters are identified by dynamics estimator. The results of calibration are shown in Tab.II.

B. Results of Position Control

The experiments of position control is taken on the hip joint of the robot by swinging the leg from one demanded position to another. To implement the algorithm in the system, in which the second order deviation of θ_h engenders large noise and introduces oscillation, an identified equation of (1) is used to estimate the acceleration $\ddot{\theta}_h$. Two experiments are compared to validate the effectiveness of the position controller. One is an experiment of position controller with no active damping($\lambda_1 = 0$), and another is of position controller with proper active damping ratio($\lambda_1 = 30$).

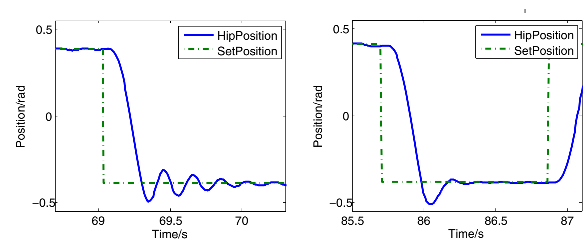

(a) (b)

Fig. 8: (a)Position controller without active damping; (b)Position controller with active damping

The experimental result is shown in Fig.8. Due to the active damping the controller generates, the joint can move fast from one position to the demanded one and absorb extra energy in spring instantly. Otherwise, with the position controller without active damping the joint should dissipate its extra energy during moving by its passive damping, which causes oscillations in the joint.

C. Results of Body Balance Maintenance

To validate the effectiveness of body maintenance algorithm, consecutive hopping experiment is taken on the single leg robot. To get the dynamics function $f(.)$ for body balance maintenance, sampled data and fitted curve are shown in Fig.9. Following form is used to fit the sampled data:

$$f(x) = a_0 + a_1 x + a_2 x^2 + a_3 x^3 \tag{27}$$

in which the value of a_0 to a_3 are calculated by least square algorithm. These values are shown in Tab.III. By learning the curve from experiments, the demanded value of torque integration during stance phase can be calculated from inverse function of the curve.

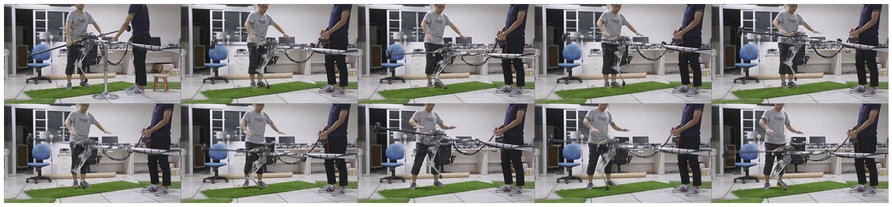

Fig. 10: Snapshot of Hopping Experiment

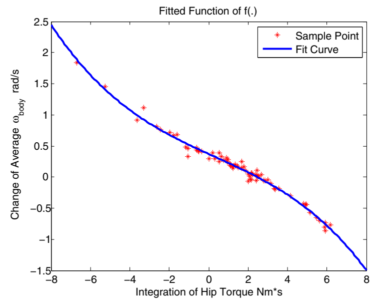

Fig. 9: Fitted relationship between the integration of hip torque during stance phase and change of average angular velocity during flight phase

TABLE III: Coefficients of fitted function

a_0	0.3708	a_1	-0.1445
a_2	0.0016	a_3	-0.0016

In this experiment, the robot successfully hops for several times without tipping its body. The snapshots of the experiment are shown in Fig.10 and the video of experiment result can be found in https://v.qq.com/x/page/s0382oilrnc.html. Data of robot during consecutive hopping are shown in Fig.11.The curve of $pitch_{body}$ shows that the pitch of robot body is maintained among -1.5 degree to 4 degree during consecutive hopping. The noise of angular velocity measurement ω_{body} is too strong to implement a traditional PD controller. The integration value of torque during each stance phase and average angular velocity of body during each flight phase are shown in Fig.12. The plot demonstrates that the integration value of torque always reach the demanded value during each hop by applying the proposed online torque planner. The output of precise torque integration, the average angular velocity of body is maintained. From the curve of hip torque during stance phase in Fig.13, the benefits of introducing integration form to control are shown: (1)although an impact occurs in hip joint after the robot crashes to the ground, the online torque planner compensates the influence of impact and reach the demanded integration value; (2)although inaccuracy and substantial delay exist in torque output of hip joint, the torque planning algorithm suppress the ultimate error in torque integration.

The power curve of motor and joint during stance phase shown in Fig.14b demonstrates that the hopping recycles the energy and achieves energy efficiency. The whole energy a motor need to inject to the system W_{motor} is $8.3339J$, and

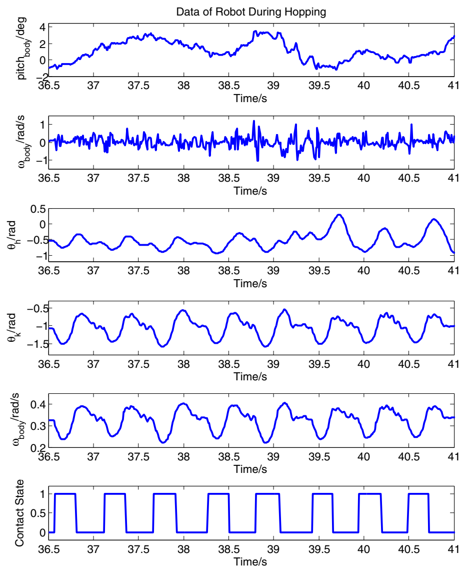

Fig. 11: Data of robot during consecutive hopping

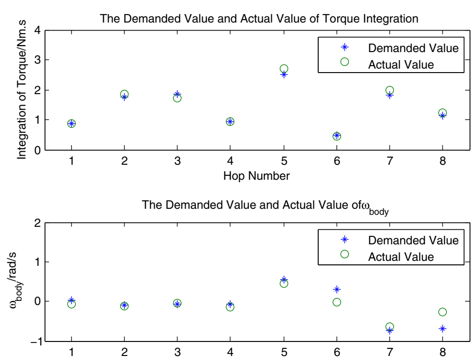

Fig. 12: The integration of hip torque and average angular velocity of robot body in each hop

the output energy of knee joint W_{knee} is $21.4334J$ during stretch phase. Hence, $13.0995J$ energy is stored in one hop. The energy efficiency is calculated by the equation in [17]:

$$\eta = \frac{W_{knee} - W_{motor}}{W_{knee}} \tag{28}$$

The calculated efficiency η is 0.612 during one hop, which is close to the efficient hopping robot of [17].

VI. CONCLUSIONS

This paper introduces the design of an SEA based single leg robot, and proposes algorithms to achieve stable and

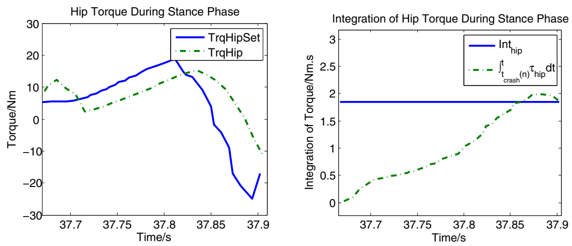

(a) (b)

Fig. 13: (a)Torque of hip joint during stance phase; (b)Integration of hip torque during stance phase

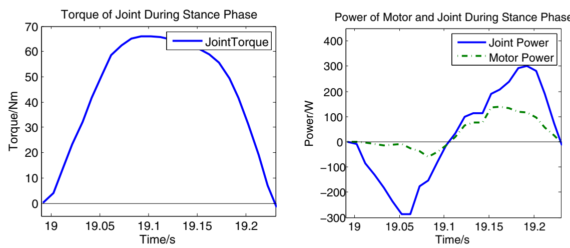

(a) (b)

Fig. 14: (a)Torque of knee joint during stance phase; (b)Power of knee joint and knee motor during stance phase

efficient hopping in consideration of the limitations of SEA. Resorting to online and offline identifications, these algorithms are auto tuned and stable hopping is implemented on a practical system. However, due to the limitations of the SEA actuator in hip joint, the velocity of hopping is still not controlled precisely due to the imprecise foot hold of the robot during consecutive hopping. Hence, beside the active damping a position controller generates, extra damping mechanism on SEA joints is still demanded for a more controllable hopping robot with SEA joints. Future work will extend the proposed algorithms in bipedal robots to implement efficient locomotion.

References

[1] T.Y. Wu, T.J. Yeh and B.H. Hsu, "Trajectory Planning of a One-Legged Robot Performing a Stable Hop", *The International Journal of Robotics Research*, vol.30, no.8, pp.1072–1091, 2011.

[2] R. Tajima, K. Suga, "Motion having a Flight Phase: Experiments Involving a One-legged Robot", *International Conference on Intelligent Robots and Systems(IROS)*, IEEE, 2006, pp.1726–1731

[3] M. Raibert, K. Blankespoor, G. Nelson, and R. Playter, "BigDog, the rough-terrain quadruped robot", in *Proc. 17th World Congress*, 2008, pp. 10823C-10825.

[4] Boston Dynamics. (2012). [Online]. Available: http://www. bostondynamics.com, 2012.

[5] C. Semini, N. G. Tsagarakis, E. Guglielmino, M. Focchi, F. Cannella, and D. G. Caldwell, "Design of HyQłA hydraulically and electrically actuated quadruped robot", *Mech. Eng., Part I, J. Syst. Control Eng.*, vol. 225, no. 6, pp. 831C-849, 2011.

[6] S. Seok, A. Wang, D. Otten, and S. Kim, "Actuator design for high force proprioceptive control in fast legged locomotion", in *International Conference on Intelligent Robots and Systems(IROS)*, IEEE/RSJ 2012, pp. 1970-C1975.

[7] S. Seok, A. Wang, D. Otten, J. Lang, and S. Kim, "Design principles for highly efficient quadrupeds and implementation on the MIT Cheetah robot", in *International Conference on Robotics Automation(ICRA)*, IEEE, 2013, pp. 3307-C3312

[8] F. Iida, G. Gomez, and R. Pfeifer, "Exploiting body dynamics for controlling a running quadruped robot", *International Conference on Robotics and Automation(ICRA)*, Barcelona, Spain, 2005, pp. 229–35.

[9] S. Rutishauser, A. Sprowitz, L. Righetti, and A. J. Ijspeert, "Passive compliant quadruped robot using Central Pattern Generators for locomotion control, in *International Conference on Biomedical Robotics and Biomechatronics(BioRob)*, IEEE, 2008, pp. 710–715.

[10] J. A. Smith and I. Poulakakis, "Rotary gallop in the untethered quadrupedal robot scout II," in *International Conference on Intelligent Robots and Systems(IROS)*, IEEE/RSJ , 2004, pp. 2556–2561 vol.3.Q

[11] R. Niiyama, A. Nagakubo, Y. Kuniyoshi, "Mowgli: A Bipedal Jumping and Landing Robot with an Artificial Musculoskeletal System", *International Conference on Robotics and Automation(ICRA)*, Roma, Italy, 2007, pp. 2546–2551.

[12] S.H.Hyon, T.Mita, "Development of a Biologically Inspired Hopping Robot - *Kenken*", *International Conference on Robotics and Automation(ICRA)*, Washington, DC, 2002, pp. 3984–3991.

[13] G. Pratt and M. Williamson, "Series elastic actuators," in *International Conference on Intelligent Robots and Systems(IROS)*, Pittsburg, PA, 1995, pp. 399–406.

[14] I. Poulakakis and J. W. Grizzle, "Modeling and Control of the Monopedal Robot Thumper", *International Conference on Robotics and Automation(ICRA)*, Kobe, Japan, 2009, pp. 3327–3334.

[15] K. Sreenath, H. W. Park, I. Poulakakis and J. W. Grizzle, "Embedding active force control within the compliant hybrid zero dynamics to achieve stable, fast running on MABEL", *The International Journal of Robotics Research*, 2013, vol.32, No.3 324–346

[16] M. Hutter, C. D. Remy, M. A. Hoepflinger, and R. Siegwart, "ScarlETH: Design and Control of a Planar Running Robot", *International Conference on Intelligent Robots and Systems(IROS)*, San Francisco, 2011, pp. 562–567.

[17] M. Hutter, C. D. Remy, M. A. Hoepflinger, and R. Siegwart, "Efficient and Versatile Locomotion With Highly Compliant Legs", *IEEE/ASME Transactions on Mechatronics*, Vol.18, No.2, 2013, pp. 449–458

[18] M. Hutter, C. Gehring, M. A. Hoepflinger, M. Bloesch, and R. Siegwart, "Toward Combining Speed, Efficiency, Versatility, and Robustness in an Autonomous Quadruped", *IEEE Transactions on Robotics*, Vol. 30, No. 6, 2014, pp. 1427–1440

[19] M. Grimmer, M. Eslamy, S. Gliech and A. Seyfarth, "A Comparison of Parallel- and Series Elastic Elements in an actuator for Mimicking Human Ankle Joint in Walking and Running" , *International Conference Robotics and Automation(ICRA)*, IEEE, 2012,pp. 2035C-2040.

[20] M. Slovich, N. Paine, K. Kemper, A. Metger, A. Edinger, J. Weber, and L. Sentis, "Building HUME: A bipedal robot for human-centered hyperagility", *Dynamic Walking Meeting*, 2012.

[21] K. Radkhah, C. Maufroy, M. Maus, Scholz D, A. Seyfarth, and O. Von Stryk, "Concept and design of the biobiped1 robot for human-like walking and running", *International Journal on Humanoid Robots*, vol. 8, no. 3, pp. 439-C458, 2011.

[22] N. Tsagarakis and Z. Li, "The design of the lower body of the compliant humanoid robot cCub'", *International Conference Robotics and Automation(ICRA)*, IEEE, 2011, pp. 2035C-2040.

[23] J. Pratt and B. Krupp, "Design of a bipedal walking robot", in Unmanned Systems Technology X, pp. 69621F–1-C69621F–13, 2008.

[24] Jonathan W. Hurst and Alfred A. Rizzi, "Series Compliance for an Efficient Running Gait", *IEEE Robotics and Automation Magazine*, 2008, pp. 42–51

[25] H. R. Vejdani and J. W. Hurst, "Optimal Passive Dynamics for Physical Interaction: Throwing a Mass", *International Conference on Robotics and Automation(ICRA)*, Karlsruhe, Germany, 2013, pp. 788–793.

[26] M.Raibet: "Legged Robota That Balance", MIT Press, 1985

[27] H. Mayeda, K. Yoshida, and K. Osuka, "Base parameters of manipulator dynamic models", *IEEE Transactions on Robotic and Automation*, vol. 6, no. 3, pp. 312-C321, Jun. 1990.

[28] P. Khosla and T. Kanade, "Parameter Identification of Robot Dynamics", *24th IEEE Conference on Decision and Control*, 1985, pp. 1754–1760

[29] Jean-Jacques E. Slotine, Weiping Li. Applied nonlinear control, China Machine Press, 2004